Universal statistical properties of drift-interchange turbulence in TORPEX toroidal plasmas

B. Labit, I. Furno, A. Fasoli, A. Diallo, S.H. Müller, G. Plyushchev, M. Podestà and F.M. Poli
Centre de Recherches en Physique des Plasmas (CRPP) - École Polytechnique Fédérale de Lausanne (EFPL)
Association EURATOM-Confédération Suisse CH-1015 Lausanne, Switzerland.

A unique parabolic relation is observed to link skewness and kurtosis of around ten thousands density fluctuation signals, measured over the whole cross-section of a toroidal magnetised plasma for a broad range of experimental conditions. All the probability density functions of the measured signals, including those characterised by a negative skewness, are universally described by a special case of the Beta distribution. Fluctuations in the drift-interchange frequency range are necessary and sufficient to assure that probability density functions can be described by this specific Beta distribution.

PACS numbers: 52.25.Xz, 52.35.Ra, 52.55.Hc, 52.35.Kt

Plasma turbulence and associated anomalous transport constitute main limiting factors for the performance of magnetic fusion devices. Fluctuations leading to a turbulent state and possible methods to control them have been investigated for many years [1]. A statistical description of plasma turbulence [2] is appropriate to capture some of the underlying physical mechanisms. In particular, a significant effort is dedicated to finding universal aspects in this statistical description [3], i.e. a common behavior for all spatial and temporal scales and/or for different physical systems and experimental conditions. The knowledge of some of these universal properties may lead to a better understanding of the impact of different types of micro-instabilities on the macroscopic behavior of the plasma, e.g. in terms of fluctuation induced transport, self-similarity or intermittency. In addition, it would generalise and extend the impact of the experimental results obtained on different invidual machines. Such quest for universality is pursued in turbulence research for a variety of systems, including the Earth oceans [5] and atmosphere [4], the solar corona [6], and in magnetically correlated systems [7]. In magnetic fusion plasmas, the universality of the probability density function (PDF) is investigated in various devices and experimental conditions [8–15], only using local density measurements at the plasma edge or in the Scrape-Off-Layer (SOL). Despite the common observation that PDFs of density fluctuations are non-Gaussian, there is no consensus on a unique PDF that could model all the experiments.

In this Letter, we address the question of the universality of plasma fluctuations associated with drift-interchange turbulence by measuring statistical properties that are common to a large number of electron density signals ($\approx$ 10000), taken across the entire plasma cross-section and over a broad range of experimental conditions. The experiments are performed in TORPEX [16], a toroidal device with major and minor radius $R = 1$ m and $a = 0.2$ m, and a toroidal magnetic field up to 0.1 T. A small vertical magnetic field component ≤ 4 mT is superimposed to partly short circuit the vertical electric field due to $\nabla \underline{\mathrm{B}}$ and curvature drifts and reduce the fast particle losses [17]. Highly reproducible plasmas are created and sustained for up to 1.5 s by means of waves in the Electron Cyclotron range of frequencies [18]. Measurements of ion saturation current are obtained over the whole plasma cross-section (comprising source, edge and confinement region) in a single plasma discharge, with a spatial resolution of 3.5 cm and at a sampling frequency of 250 kHz with a hexagonal array of 86 Langmuir probes, named HEXTIP [19]. As in these experiments temperature fluctuations are small compared to density fluctuations, ion saturation current fluctuations are assumed to be directly proportional to electron density fluctuations. The microwave power and the toroidal magnetic field are kept constant, while different neutral gases are used (H, He, Ar). The vertical magnetic field and the neutral gas pressure are varied leading to variations of the ion gyro radius, the plasma shape, the ion-neutral collision frequency. As a consequence, for all signals, the range of time averaged densities $\bar{n}$ and electron temperature $\bar{T}_e$ extends between 1.4×10^{15} m^{-3} and 3.7×10^{17} m^{-3} and 1eV and 10 eV, respectively. The range of fluctuation levels is $1\% \leq \delta n/\bar{n} < 95\%$ where δn is the r.m.s. fluctuating density. The observed density fluctuations are associated with drift-interchange turbulence, generated in regions of bad field curvature and convected away by the $\underline{\mathrm{E}} \times \underline{\mathrm{B}}$ fluid motion [16, 20]. Thus, the nature of these fluctuations is relevant for edge/SOL turbulence studies, thought the achieved range of density fluctuations for instance, is large compared to what can be covered in tokamaks, even across several different devices.

Two examples of experimental signals representing the time evolution of the electron density are shown in Fig. 1(a). The top trace is characterized by bursty positive events, hence by a PDF with positive skewness (normalized third order moment of the PDF) while the bottom one displays negative bursts, corresponding to a negatively skewed distribution. For all the signals, the skewness and the kurtosis (normalized fourth order moment of the PDF) are estimated and plotted against each other [4], Fig. 1(b). We observe that a significant fraction of the signals ($\simeq 30\%$) are characterized by a negative skewness. Previous measurements in tokamak plasmas [12] reported a change in the skewness sign from positive to negative values when crossing the last closed flux surface from the SOL region into the plasma edge. The data in Fig. 1(b) is least-square fitted by the quadratic polynomial

$$K = (1.502 \pm 0.015)S^2 + (2.784 \pm 0.019). \qquad (1)$$

The uncertainty on the estimated coefficients provides the

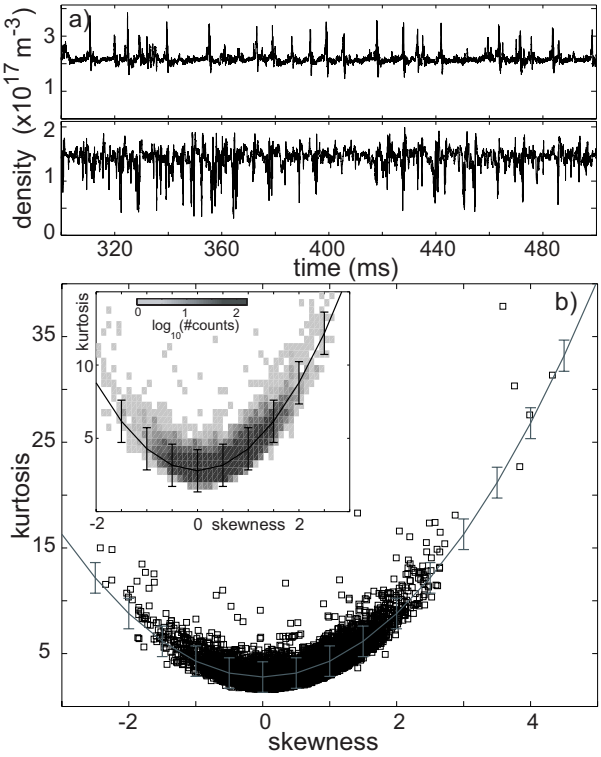

FIG. 1: a) Example of experimental signals having a positive (top) and negative (bottom) skewed distribution. b) Kurtosis *versus* skewness computed for the 8966 experimental signals. The fitting second order polynomial (solid grey line) is also plotted. Inset) Joint probability of K and S for the experimental signals. On both graphs, the error bars correspond to the 95% confidence interval.

95% confidence bounds. This interval is illustrated on the graph with error bars. The inset in Fig. 1(b) shows that approximately 95% of the experimental data is contained within these error bars. The fact that the skewness and the kurtosis of fluctuations can be characterized by a quadratic relation $K = \alpha S^2 + \beta$ has been shown in very different physical situations such as for the concentration of a pollutant diffused and convected by the turbulent atmosphere [4] or for the surface elevation of wind waves in nonlinear interactions [21]. Such a link between third and fourth order moments is valid for a large set of PDF families [22]. When this relation is satisfied, an estimate of the coefficient α would bring information of the underlying physical mechanism. This emphasizes the importance to identify a particular parabolic relation when trying to determine a theoretical PDF that reproduces experimental distributions. Because of the functional relation between the kurtosis and the skewness, all the analytical PDFs that are defined with constant S and K (normal, logistic, Rayleigh, uniform, exponential,...) cannot universally reproduce the experimental measurements. Furthermore, a quadratic polynomial rules out distributions (triangular, error, Student's,...) for which either K or S varies, but the other moment is constant. Finally, the robustness of the least-square fit Eq. (1) excludes distributions (Weibull, Log-normal, Wald, F,...) that have a similar relationship between K and S but with different coefficients [22]. The polynomial in Eq. (1) is very close to the relation between the kurtosis and the skewness associated with the Gamma distribution: $K = 1.5S^2 + 3$, although the skewness of the Gamma distribution is by definition always positive [22]. One distribution that can admit both positive and negative skewness is the Beta distribution [22]. It has a very versatile shape and is commonly used to model theoretical distributions and applied in a wide variety of situations like fecundability studies, proportions in gas mixture, risk analysis, concentration of contaminants in soil, concentration of pollutants in the atmosphere and quality control [22]. For a random variable n, the general Beta distribution is defined by:

$$F_\beta(n; p, q, n_l, n_h) = \frac{(n - n_l)^{p-1}(n_h - n)^{q-1}}{\mathcal{B}(p, q)(n_h - n_l)^{p+q-1}} \qquad (2)$$

where $n_l \leq n \leq n_h$; $p, q > 0$ and $\mathcal{B}$ is the Beta function. Its first four associated moments are defined by

$$\mu = \frac{p}{p+q}(n_h - n_l) + n_l, \qquad (3a)$$

$$\sigma^2 = \frac{pq}{(p+q)^2(p+q+1)}(n_h - n_l)^2, \qquad (3b)$$

$$S = \frac{2(q-p)}{(p+q+2)}\sqrt{\frac{p+q+1}{pq}}, \qquad (3c)$$

$$\text{and } K = \frac{3(p+q+1)\left[2(p+q)^2 + pq(p+q-6)\right]}{pq(p+q+2)(p+q+3)}. \qquad (3d)$$

The relation between the third and fourth moments is not trivial since it depends on parameters p and q, but S and K do not depend explicitly on the boundaries of the random variable n. Moreover, for any (p, q) it can be shown that [22]

$$1 + S^2(p, q) \leq K(p, q) \leq 3 + 1.5S^2(p, q). \qquad (4)$$

The upper limit is reached when $q \to +\infty$ for positive skewness and when $p \to +\infty$ for negative skewness. The Beta distribution tends to the Gamma distribution when $n_h \to +\infty$ together with $q \to +\infty$. The experimentally measured skewness and kurtosis are very close to the upper limit of the domain of variation for a Beta distribution, thus either p or q has to be large.

According to Eq. (2), the Beta distribution is defined with four parameters: p, q, n_l and n_h. One specificity of this distribution is the bounded range of variation of the random variable. This is compatible with the variation of the plasma density which is necessarily bounded between zero (no plasma) and the neutral gas density (fully ionized plasma). Nevertheless, for each experimental time series, we restrict this range of variation by the following choice $n_l = n_{\min}$ and $n_h = n_{\max}$ where $n_{\min}$ and $n_{\max}$ are the minimum and the maximum of each signal. This choice implies $F(n < n_{\min}) = F(n > n_{\max}) = 0$ where $F(n)$ is the experimental probability density function, and can be partly justified by the statistical stationarity of the signals. Fig. 2(a) represents the maximum and minimum of a given signal obtained for increasing portions of the whole time series plotted as a function

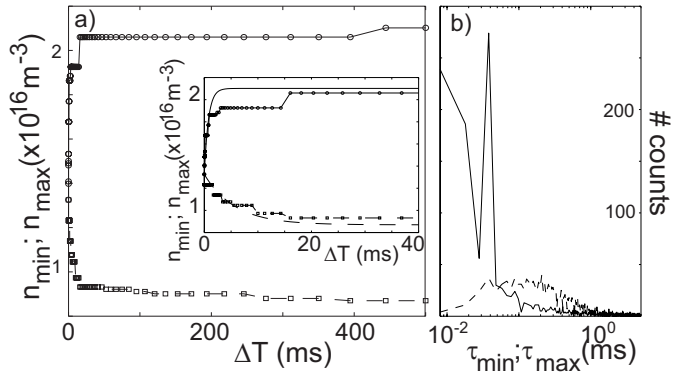

FIG. 2: a) Maximum (○) and minimum (□) of an experimental signal for different time series durations, ΔT. Their variation can be approximated with an exponential fit (inset). b) Distribution of the characteristic times for the maxima $\tau_{\max}$ (solid) and for the minima $\tau_{\min}$ (dashed) for a subset of 2434 signals. Most of them are much shorter than the complete time series duration.

of the duration of such portions, ΔT. After a fast variation at small time series duration ($\Delta T \leq 1$ ms), the minimum and the maximum are slowly varying. In order to show that our time series duration is sufficiently long to reach a statistical stationarity, the time evolution of $n_{\min}$ or $n_{\max}$ is fitted by an exponential characterized by a time constant τ. The histogram of the two time constants for a subset of approximately 2500 signals is plotted on Fig. 2(b). Almost all the time constants are smaller than 1 ms, which is much shorter than the complete time record of the signals. The statistical stationarity of the experimental data is also reflected in the fact that the two coefficients in Eq. 1 change only by $\sim 3\%$ as the time series is shortened down to 10 ms.

Having fixed the upper and lower boundaries for each signal, only two free parameters, p and q, remain for the Beta distribution. These are estimated by inverting Eqs. (3a-3b) and inserting the experimental values of the mean, variance, minimum and maximum of each signal:

$$p = \bar{\mu}\left[\frac{\bar{\mu}(1-\bar{\mu})}{\bar{\sigma}^2} - 1\right] \text{ and } q = (1-\bar{\mu})\left[\frac{\bar{\mu}(1-\bar{\mu})}{\bar{\sigma}^2} - 1\right] \quad (5)$$

with $\bar{\mu} = \dfrac{\mu_{\exp} - n_{\min}}{n_{\max} - n_{\min}}$ and $\bar{\sigma}^2 = \dfrac{\sigma_{\exp}^2}{(n_{\max} - n_{\min})^2}$. The joint distribution of the estimated parameters p and q is represented on Fig. 3(a). These parameters are large (typically > 100), thus S and K for a Beta distribution, Eqs. (3c-3d), are close to the upper limit in Eq. (4) and are compatible with the experimental third and fourth moments. A posteriori, our choice for parameters n_l and n_h can be further justified by the fact that a non negligible fraction of negative skewness, estimated for a Beta PDF with these p and q is conserved. Setting $n_h \to +\infty$ would exclude negative skewness and setting $n_l = 0$ would artificially increase the fraction of negative skewness.

An illustration of the good agreement between the experimental PDF and the Beta distribution is shown in Fig. 3(b-c) for a negative and a positive skewed experimental

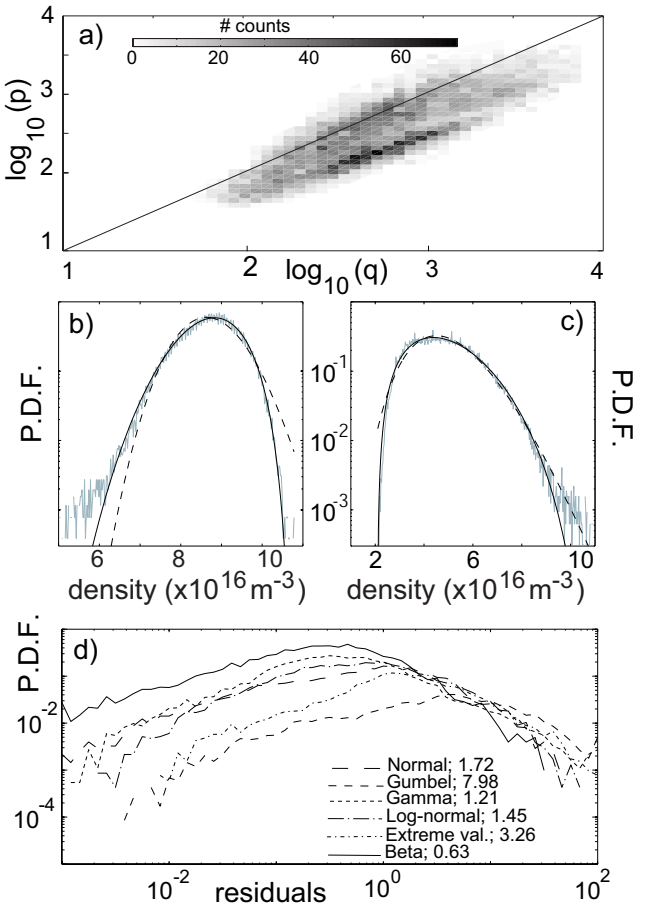

FIG. 3: a) Joint distribution of parameters p and q estimated with $\mu_{\exp}$, $\sigma_{\exp}$, $n_{\min}$ and $n_{\max}$. b) and c) Two experimental distributions from Argon plasmas (gray line) with a negative (b) and positive (c) skewness. The Beta distribution (solid) and the Gamma distribution (dash) estimated with $\mu_{\exp}$ and $\sigma_{\exp}$ are also plotted. d) Distributions of the residuals between all the experimental PDFs and several analytical distributions estimated with $\mu_{\exp}$ and $\sigma_{\exp}$. The average value of the residuals is indicated in the legend.

distributions. For all the signals, we compute the residual $r_j \equiv \sum_n (F(n) - F_j(n))^2$ between the experimental distribution $F(n)$ and several analytical PDFs $F_j(n)$, including the Beta distribution, estimated with $\mu_{\exp}$ and $\sigma_{\exp}$. The probability distribution function of the residuals is shown in Fig. 3(d). The Beta distribution provides the smallest average residual as well as a better fit than any other tested PDFs in the region of small residuals ($r_j \leq 0.1$). All the experimental PDFs can be universally reproduced by a limiting case of the Beta distribution. In this limit, the Beta distribution is equivalent to $F_\Gamma(n)$ for positive skewness and to $F_\Gamma(2\mu - n)$ for negative skewness, where μ is the mean value of the density n and F_Γ is the Gamma distribution defined by $F_\Gamma(n) = \theta^{-\alpha} n^{\alpha-1} \mathrm{e}^{-n/\theta}/\Gamma(\alpha)$ [22]. The Gamma distribution has previously reported to be compatible with the PDF of experimental signals measured in the SOL of a tokamak and characterised by positive skewness [14].

Having established the existence of a universal PDF shape

that describes the experimental distributions, we address the question of which physical mechanisms contribute to such behaviour. In particular, we investigate which frequency range of the fluctuations spectrum, if any, is necessary and sufficient to recover the Beta distribution. For the three neutral gases used, approximately 800 signals have been filtered at different cut-off frequencies (0.1 kHz $\leq f_c \leq 50$ kHz) with both low-pass and high-pass filters. For all the cut-off frequencies, the skewness and the kurtosis of the filtered signals are estimated. For each f_c, the residual between the kurtosis $K(f_c)$ and the values estimated for the skewness $S(f_c)$ with Eq. (1) is computed and normalized to the original residual for the unfiltered signals, Fig. 4(a). As f_c increases (decreases) for the low-pass (high-pass) filters, the difference between the original moments and those associated with filtered signals tends to disappear. For the three gases, if only the low ($f_c \leq 1$ kHz) or high ($f_c \geq 20$ kHz) frequency contributions to fluctuations are kept, the experimental fit described by Eq. 1 cannot be satisfied. In addition, the difference between the plasmas made from different neutral gases are reflected in the averaged spectra normalized to the integral of the spectra between 0 and 125 kHz, Fig. 4(b). The density fluctuations contained in the measured frequency range of drift-wave instabilities (1 kHz $\leq f \leq 10$ kHz) [20] must be retained to recover this Beta distribution. Note that no extension to broader special regions is necessary, ruling out an interpretation of the fluctuations statistical properties as the result of a fully developed turbulence.

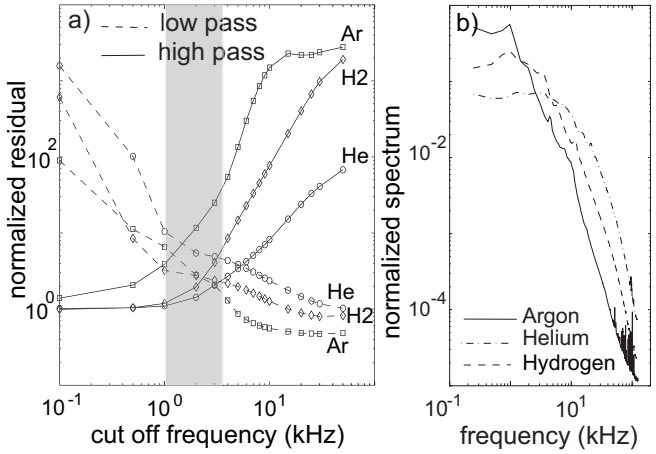

FIG. 4: a) Normalized residuals for different cut-off frequencies of a low-pass and a high-pass filters. b) Normalized averaged spectra for the three neutral gases.

In summary, we have analyzed electrostatic fluctuations measured over the entire cross-section of a simple toroidal magnetized plasma, including the source region for instabilities, regions where nonlinear mode coupling takes place and regions where the unstable modes are convected by the $\underline{\mathrm{E}} \times \underline{\mathrm{B}}$ flow. The PDF of the density fluctuations at all locations is found to have a universal character, in the sense that a unique relation links the skewness and the kurtosis , and that it can be described by the same analytical distribution. This is a special case of the general Beta distribution $F_\beta(x)$, taking the form of the Gamma distribution F_Γ, depending on the sign of the signal skewness, evaluated as follows: $F_\Gamma(x)$ for $S > 0$ or $F_\Gamma(2\bar{x} - x)$ for $S < 0$. These observations are consistent with the picture of a unique physical mechanism producing events that would generate in the same region positive and negative density structures, corresponding to a local excess of density, and a density depletion, respectively [23, 24]. Both kinds of structures would carry along their motion the same PDF features, as they originate from the same local event. Fluctuations in the typical range of frequency associated with drift wave turbulence are necessary to assure that probability density functions can be described by this specific Beta distribution. A more complete physical understanding of plasma turbulence in the present experiments requires extensive self-consistent numerical simulations of drift-interchange turbulence using nonlinear equations, e. g. based on the Hasegawa-Wakatani model. Nevertheless, the present results may have two consequences on the study of the underlying physics: the unique relation between moments of the plasma density PDF may lead to a low-order statistical closure of the chain of coupled equations [2]; the same global characterization of the statistical properties of fluctuations, applied to numerical simulations outputs, provides a valuable tool for the validation of the physical basis of the simulation model.

This work is partly funded by the Fonds National Suisse de la Recherche Scientifique. Fruitful discussions with Prof. F. Skiff and Dr. J. P. Graves are acknowledged.

[1] W. Horton, Physics Reports, **192**, 1 (1990).
[2] J.A. Krommes, Physics Reports, **360**, 1 (2002).
[3] U. Frisch, *Turbulence, The Legacy of A. N. Kolmogorov* (Cambridge University Press, 1995).
[4] P.C. Chatwin, D.M. Lewis and N. Mole, Adv. Comput. Math., **6**, 227 (1996).
[5] M.A Srokosz, J. Phys. Oceanogr., **28**, 149 (1998).
[6] L. de Arcangelis, C. Godano, E. Lippiello and M. Nicodemi, Phys. Rev. Lett., **96**, 051102 (2006).
[7] S. T. Bramwell *et al.*, Phys. Rev. Lett., **84**, 3744 (2000).
[8] B. van Milligen *et al.*, Phys. Plasmas **12**, 052507 (2005).
[9] B.A. Carreras *et al.*, Phys. Rev. Lett., **83**, 3653 (1999).
[10] G.Y. Antar *et al.*, Phys. Rev. Lett., **87**, 065001 (2001).
[11] G.Y. Antar *et al.*, Phys. Plasmas, **10**, 419 (2003).
[12] J. A. Boedo *et al.*, Phys. Plasmas, **10**, 1670 (2003).
[13] F. Sattin, N. Vianello and M. Valisa, Phys. Plasmas, **11**, 5032 (2004).
[14] J. P. Graves, J. Horacek, R.A. Pitts and K. I. Hopcraft, Plasma Phys. Control. Fusion, **47**, L1 (2005).
[15] F. Sattin *et al.*, Plasma Phys. Control. Fusion, **48**, 1033 (2006).
[16] A. Fasoli *et al.*, Phys. Plasmas, **13**, 055903 (2006).
[17] S. H. Müller *et al.*, Phys. Rev. Lett., **93**, 165003 (2004).
[18] M. Podestà *et al.*, Plasma Phys. Control. Fusion, **47**, 1989 (2005); **48**, 1053 (2006).
[19] S.H. Müller *et al.*, Phys. Plasmas, **12**, 090906 (2005).
[20] F.M. Poli *et al.*, Phys. Plasmas, **13**, 102104 (2006).
[21] M. Hatori, J. Oceanogr. Soc. Japan, 40, 1 (1984).

[22] N.L. Johnson, S. Kotz and N. Balakrishnan, *Continuous univariate distributions* (John Wiley & Sons Inc, 1995), 2nd Ed.
[23] S.H. Müller *et al.*, Phys. Plasmas, **13**, 100701 (2006).
[24] T.A. Carter, Phys. Plasmas, **13**, 010701 (2006).